Tetrahedron Letters 56 (2015) 3368–3372

Contents lists available at ScienceDirect

Tetrahedron Letters

journal homepage: www.elsevier.com/locate/tetlet

Gold–copper alloyed nanorods for metal-catalyzed organic reactions: implication of surface ligands on nanoparticle-based heterogeneous catalysis ☆

Samir V. Jenkins, Shutang Chen, Jingyi Chen *

Department of Chemistry and Biochemistry, University of Arkansas, Fayetteville, AR 72701, United States

ARTICLE INFO

Article history:
Received 2 December 2014
Revised 4 March 2015
Accepted 10 March 2015
Available online 20 March 2015

Keywords:
Nanocatalyst
Nitrophenol reduction
Benzonitrile hydration
Click chemistry

ABSTRACT

Recent advances in nanoparticle synthesis have created new potential avenues for aqueous catalysis of organic reactions. Morphological control of metal nanoparticles often involves the use of surface ligands, which in turn affect the catalytic activity of nanocatalysts. This Letter demonstrates that surface anchoring group, chain length, and configuration of the water-soluble, polymeric ligands influence the catalytic properties of alloyed $AuCu_3$ nanorods for metal-catalyzed organic reactions. Due to the binding affinity of the surface-anchoring groups, a thiol anchor was found to be detrimental the Au-catalyzed reduction of *p*-nitrophenol while the Cu-catalyzed azide–alkyne cycloaddition was severely inhibited by amine anchors. Furthermore, the catalytic activity of nanorods increased with increased dimension of the ligands with the same anchoring group due to the reduction of graft density. Elevated temperature facilitates the mobility of surface ligands in benzonitrile hydration to benzamide, resulting in the enhancement of catalytic activity. This work highlights the paramount importance of surface ligand selection in the design of nanocatalysts for catalytic organic reactions.

© 2015 Elsevier Ltd. All rights reserved.

Metal nanoparticles have received considerable attention as heterogeneous catalysts in the past two decades due to their extremely large surface-to-volume ratio compared to their bulk counterparts.[1] Uniform nanoparticle suspensions are considered as the bridge between traditional homogenous and heterogeneous catalysis. Nanoparticle catalysts have demonstrated the capacity to catalyze reactions in H_2O, at relatively low temperatures, under normal atmosphere.[2] These catalysts can be readily recovered by centrifugation, therefore they can be recycled. Numerous efforts have been made to synthesize metal nanoparticles with controllable size and shape which, in turn, tune their catalytic activity.[3] In order to manipulate the morphology, surface ligands are deployed in the synthesis and the resultant nanoparticles are capped by a monolayer of these ligands. The binding affinity of these ligands to the surface plays an important role in the catalytic activity of the nanoparticles in heterogeneous catalysis because the reactant molecules are activated on the nanoparticle surface.[4–6] Ligand exchange is used as the first step in many phase transfer processes designed to retain surface activity of nanomaterials. In this Letter, we correlate the catalytic activities of aqueous, surface-capped Au–Cu alloyed nanorods to polymeric ligands with different functional groups, molecular weights, and configurations for organic reactions. This correlation allows us to choose and design surface ligand to retain and further enhance the catalytic activity of the nanoparticles.

Coinage metals, such as Au and Cu, have been demonstrated for numerous catalytic processes.[1] Alloying Au and Cu enables synergy of their catalytic properties, and thus Au–Cu alloys are better catalysts than Au or Cu alone for many important reactions such as CO oxidation,[7] propene epoxidation,[8] and benzyl alcohol oxidation.[9] Additionally, using these alloys can defray the cost of pure Au materials and reduce the reactivity of Cu with air.[10] The catalytic activity can be further altered by modifying the morphology of the nanoparticles. For example, we have demonstrated that the rod-shaped $AuCu_3$ nanoparticles are approximately ten-fold more active than spherical nanoparticles with the same composition and surface area.[11] The $AuCu_3$ nanoparticles absorb visible or near-infrared light, which may generate singlet oxygen,[12] which could be used in an alternative approach for organic syntheses developed by Prof. Harry Wasserman,[13] including bipyrrole aldehyde,[14] an intermediate in the total synthesis of prodigiosenes.[15,16] Herein, we use the $AuCu_3$ nanorods ($AuCu_3$NRs) as model catalysts to study the influence of surface ligands on their

☆ In the memory of Professor Harry H. Wasserman who was an outstanding organic chemist and inspiring educator.

* Corresponding author. Tel.: +1 (479) 575 6203; fax: +1 (479) 575 4049.
E-mail address: chenj@uark.edu (J. Chen).

http://dx.doi.org/10.1016/j.tetlet.2015.03.041
0040-4039/© 2015 Elsevier Ltd. All rights reserved.

catalytic activity. Three metal-catalyzed reactions are chosen for this study: Au-catalyzed *p*-nitrophenol reduction, Cu-catalyzed alkyne–azide 'click' cycloaddition, and metal-catalyzed nitrile hydration, all of which are important reactions for the synthesis of intermediates in drug discovery. The binding affinity of polymeric ligands to Au and Cu surfaces is correlated to their catalytic activity for these three reactions.

The $AuCu_3$NRs were synthesized by alkylamine reduction as previously described.[11] Briefly, $HAuCl_4$ was reduced at 140 °C for 20 min in tetradecylamine under protection of Ar to generate Au seed particles. The reaction temperature was increased to 210 °C and copper acetylacetonate (4:1 mol ratio Cu–Au) dissolved in oleylamine was injected. The reaction was allowed to proceed for another 20 min to form $AuCu_3$NRs. Figure 1A shows the transmission electron microscopy (TEM) image of typical $AuCu_3$NRs, having an average length of 25.0 ± 2.1 nm and diameter of 11.2 ± 1.0 nm, equal to an aspect ratio of ~2. The powder X-ray diffraction (XRD) pattern verified that the $AuCu_3$NRs adopted face-centered-cubic (fcc) crystal structure, suggesting a random alloy of Au and Cu (Fig. 1B). The peaks at 42.1, 48.2, and 71.3 °C were assigned to (111), (200), and (220) crystallographic planes of fcc structure. The composition (1:3 ratio Au to Cu) of the $AuCu_3$NRs was confirmed by analyzing the most prominent peak of the (111) plane using Vegard's law. Figure 1C shows the optical spectrum of the $AuCu_3$NRs with an extinction peak at 670 nm. To obtain water-soluble catalysts, ligand exchange was performed in $CHCl_3$, followed by transferring into aqueous solution using ethanol as a phase transfer intermediary.[11,17] After phase transfer, the $AuCu_3$NRs were well-dispersed in aqueous solution and there was little change in their optical spectra. The concentrations of Au and Cu were measured by flame atomic absorbance spectroscopy.

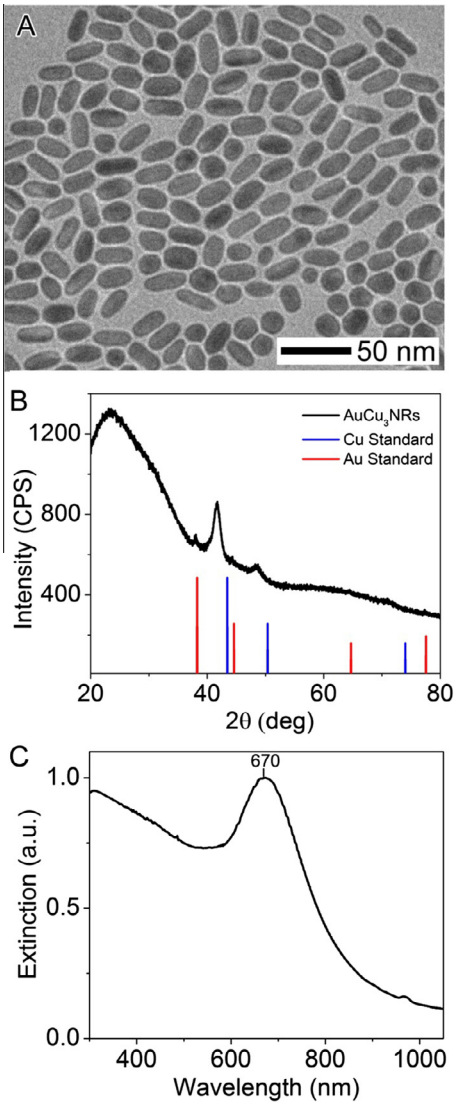

Figure 1. Characterization of $AuCu_3$NRs: (A) TEM image; (B) XRD pattern; and (C) extinction spectrum.

Water-soluble polymers were used to replace the alkylamines capping the surface of the $AuCu_3$NRs, yielding water-soluble catalysts. Table 1 lists the water-soluble polymers including linear poly(ethylene glycol) (PEG) and branched poly(ethyleneimine) (PEI). PEG (M.W. = 5000) terminated with amine (–NH_2), thiol (–SH), and carboxylic acid (–COOH) functional groups were chosen for the study, named as PEG-NH_2, PEG-SH, or PEG-COOH. The amine group has a high affinity to coordinate with Cu while the thiol group strongly interacts with Au surface. The carboxylic acid group loosely attaches to both Cu and Au surfaces. The effect of multidentate binding to the surface is compared using PEI which contains multiple amino groups. The influence of steric hindrance is studied using PEG and PEI with different molecular weights. To investigate the effects of capping-ligand effects on the catalytic properties, Au-catalyzed *p*-nitrophenol reduction, Cu-catalyzed alkyne–azide 'click' cycloaddition, and metal-catalyzed nitrile hydration were selected to test the hypotheses.

The $NaBH_4$ reduction of *p*-nitrophenol (more accurately, *p*-nitrophenolate) is a well-studied model reaction for nanoparticle-based catalysis (Scheme 1).[18] Compared to Cu, Au can catalyze the *p*-nitrophenol reduction more efficiently.[19] The reduction process can be monitored by the loss of absorbance at 400 nm corresponding to the disappearance of *p*-nitrophenolate.[19] The reaction proceeds through two steps: an induction period (t_0) wherein the surface of the particle is reconstructed to activate the adsorbed reactant molecules and a catalytic period (k_{cat}) where the reaction follows first-order kinetics with respect to *p*-nitrophenol concentration.[20] In the absence of metal nanoparticles the reaction had not proceeded after 2 h incubation (Fig. S1). Table 2 lists the results derived from the UV–vis spectroscopic analysis. Figure 2 shows the UV–vis spectroscopic monitoring of the reaction process in the presence of ligand-capped $AuCu_3$NRs. The induction period was found to be 3.7, 3.9, and 17.7 min for the PEG-NH_2, PEG-COOH, and PEG-SH and the k_{cat} (s^{-1}) was determined to be 0.0048, 0.0033, and 0.0022, respectively, for 1 ppm Au samples (catalyst

Table 1
Summary of aqueous $AuCu_3$NRs capped by different polymeric ligands

$AuCu_3$NR sample name	Ligand	Terminus	M.W. (KDa)	Au/Cu (mol/mol)
PEG-NH_2	Poly(ethylene glycol)	–NH_2	5000	0.41
PEG750	Poly(ethylene glycol)	–NH_2	750	0.40
PEG-SH	Poly(ethylene glycol)	–SH	5000	0.46
PEG-COOH	Poly(ethylene glycol)	–COOH	5000	0.43
PEI10000	Poly(ethyleneimine)	Branched, –NH_2	10000	0.55
PEI600	Poly(ethyleneimine)	Branched, –NH_2	600	0.54

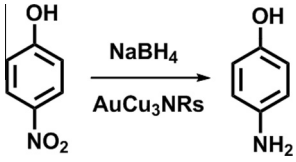

Scheme 1. Au-catalyzed *p*-nitrophenol reduction.

Table 2
Catalytic efficiency of ligand-capped $AuCu_3NRs$ for *p*-nitrophenol reduction

Sample	[Au] (ppm)	k_{cat}[a] (s^{-1})	t_0[b] (min)
PEG-NH_2	1.0	0.0048	3.7
PEG-COOH	1.0	0.0033	3.9
PEG-SH	1.0	0.0022	17.7
PEG-NH_2	2.0	0.0101	0.9
PEG750	2.0	0.0062	1.4
PEI10000	2.0	0.0071	2.3
PEI600	2.0	0.0064	2.0

[a] Determined by taking the slope of the linear portion of $\ln(Abs_0/Abs)$.
[b] Determined by minimum in 1st derivative of Abs versus time.

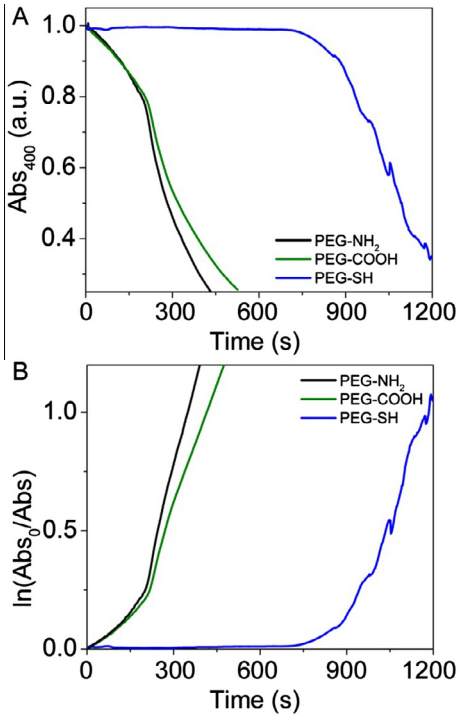

Figure 2. Nitrophenol reduction catalyzed by (black) PEG-NH_2, (green) PEG-COOH, and (blue) PEG-SH monitored as (A) absorbance at 400 nm, and (B) natural log of the ratio of absorbance at 400 nm at time = 0 and time = *t*.

loading 1% by Au atom). The strong binding between the thiol and Au prevents access of reactant molecules to the metal surface.[6] As a result, the induction time is increased and the k_{cat} reduces. On the other hand, the $AuCu_3NRs$ with weakly-bound PEG-NH_2 and PEG-COOH show much shorter induction times and larger catalytic rate constants than those with tightly-bound PEG-SH.

Several different polymers with amine groups were used to investigate the effects of multidentate binding and steric hindrance, as shown in Figure 3. Both PEG750 and PEG-NH_2 provide a single anchor to the $AuCu_3NR$ surface, while the PEIs allow multidentate binding to the metal surface. Using 2 ppm Au (2% catalyst loading) the induction times were 1.4 and 0.8 min and the k_{cat} were 0.0062 and 0.0101 s^{-1} for PEG750 and PEG-NH_2 capped $AuCu_3NRs$, respectively. This discrepancy can be attributed to the increased graft density of shorter polymers relative to longer polymers,[21] thereby inhibiting the access of reactants to active sites on the surface. The PEI-capped $AuCu_3NRs$ showed induction times of 2.3 and 2.0 min and k_{cat} of 0.0064 and 0.0071 s^{-1} for PEI600 and PEI10000, respectively. One would expect that the multidentate binding ligands should greatly reduce the catalytic activity; however, the catalytic activity of PEI600-capped

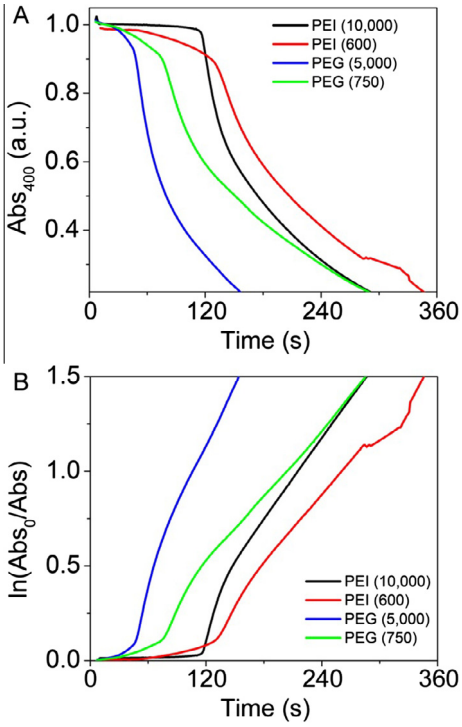

Figure 3. Nitrophenol reduction catalyzed by (black) PEI10000, (red) PEI600, (blue) PEG-NH_2, and (green) PEG750 monitored as (A) absorbance at 400 nm, and (B) natural log of the ratio of absorbance at 400 nm at time = 0 and time = *t*.

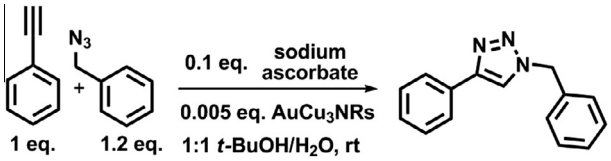

Scheme 2. Cu-catalyzed alkyne–azide 'click' cycloaddition.

Table 3
Catalytic efficiency of ligand-capped $AuCu_3NRs$ for azide–alkyne cycloaddition

Catalyst	0.5 h conversion[a]	2 h conversion[a]	18 h conversion[a]
No catalyst	<2%	<2%	<2%
CuCl	5%	20%	>98%
PEG-NH_2	<2%	<2%	<2%
PEG750	<2%	6%	51%
PEG-SH	2%	15%	>98%
PEG-COOH	2%	11%	>98%
PEI10000	3%	16%	>98%
PEI600	6%	19%	>98%

[a] Determined by ^1H NMR peak integrals. The reaction proceeded according to Scheme 2.

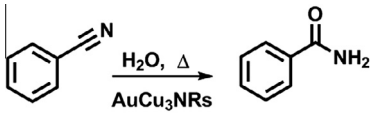

Scheme 3. Metal-catalyzed nitrile hydration.

$AuCu_3NRs$ is comparable to that of PEG750-capped ones. Coincidently, it was found that a blue supernatant was recovered during the phase transfer process with PEIs, suggesting that Cu^{2+} ions had been released from the $AuCu_3NRs$. The FAAS results

Table 4
Catalytic efficiency of ligand-capped $AuCu_3$NRs for benzonitrile hydration

Catalyst	24 h, 75 °C[a,b]	3 h, 75 °C[b]	24 h, 75 °C[b]	TOF[c] (mol/molcat h)	3 h, 95 °C[b]	TOF[d] (mol/molcat h)
No catalyst	<2%	<2%	<2%	N/A	20.7%	1380
PEG-NH_2	<2%	3.1%	14.5%	121	26.7%	1780
PEG750	<2%	8.6%	25.0%	209	40.0%	2670
PEG-SH	<2%	2.4%	10.1%	84	23.1%	1540
PEG-COOH	<2%	<2%	12.5%	104	21.2%	1420
PEI10000	3.0%	3.0%	15.1%	180	39.6%	2640
PEI600	4.6%	6.5%	21.7%	126	43.3%	2890

[a] Controls performed without $AuCu_3$NRs using 1 mg/mL ligand concentration.
[b] Conversion determined by UPLC monitoring 254 nm. Reaction proceeded according to Scheme 3 with 9.3 mM benzonitrile and 0.5 % catalyst loading.
[c] Turnover frequency calculated based on 24 h incubation.
[d] Turnover frequency calculated based on 3 h incubation.

confirmed the substantial increase in the mole fraction of Au and Cu in the $AuCu_3$NRs while XRD pattern revealed the composition remained to be $AuCu_3$. These data imply that the PEI-capped $AuCu_3$NRs are covered by a skin of pure Au, which promotes the catalytic properties of the $AuCu_3$NRs and compensates the detrimental effect of multidentate binding to the surface. The PEI etching of Cu from the $AuCu_3$NRs is akin to the Tumbaga processing that Native Americans used to produce alloyed $AuCu_3$ pots with a pure Au surface.[22] Similar to the case of PEG, the catalytic activity increased with increased chain length, suggesting that the bulky PEI10000 configuration wrapping around the $AuCu_3$NRs creates more available reaction sites compared to the smaller ligand.

To further elucidate the surface ligand effects on the bimetallic catalysts, the catalytic activity of $AuCu_3$NRs was investigated for the Cu-catalyzed 'click' reaction between benzylazide and phenylacetylene yielding a triazole (Scheme 2).[23] Pure Cu nanoparticles have been demonstrated for this reaction in THF;[24] however, the possibility of surface oxidation of the Cu nanoparticles could not be ruled out. This reaction has been demonstrated on the Au (1 1 1) surface, but the Au acts as a two-dimensional constraint rather than as a catalytic participator.[25] In this study, the click reaction was carried out in 1:1 *t*-butanol–H_2O at room temperature for 0.5, 2, and 18 h with 1 equiv phenylacetylene, 1.2 equiv benzylazide, 0.1 equiv sodium ascorbate, and 0.005 equiv Cu (as $AuCu_3$NR or CuCl, 0.5% catalyst loading). The product was isolated by extraction with dichloromethane and the conversion was quantified by ^{1}H NMR by monitoring the loss of alkyne peak (2.9 ppm) and the emergence of the vinyl peak (7.65 ppm), as listed in Table S1). No reaction was observed in the absence of Cu-based catalysts. The conversion efficiencies of the different ligand-capped $AuCu_3$NRs are included in Table 3. Comparable to the Cu^I salt as a positive control catalyst, PEG-SH and PEG-COOH capped $AuCu_3$NRs demonstrated nearly a complete conversion of phenylacetylene because the weak ligand bound surface are accessible to the reactants. The amine terminated PEG750 capped $AuCu_3$NRs only demonstrated approximately 50% conversion and PEG-NH_2 capped $AuCu_3$NRs showed almost no catalytic activity. This result indicates that the strong interaction between amines and Cu prevents successful adsorption of the reactants to the nanoparticle, thereby inhibiting the reactions. Surprisingly, both PEI750 and PEI10000, which contain numerous primary, secondary, and tertiary amines, did not seem to interfere with the catalytic process, suggesting that the leaching of Cu from $AuCu_3$NR surface weakens the binding of branched PEI to the surface and makes it available for reactants to adsorb over a prolonged reaction time. Similar trends for the ligand effects were found at the time points of 0.5 and 2 h compared to the results from 18 h.

The binding affinity of ligand to the surface is weakened as the temperature increases. To study the temperature effects on the ligand binding, the metal-catalyzed hydration of benzonitrile to benzamide was investigated (Scheme 3).[26] The reaction was run at both 75 °C and 95 °C and catalyzed using $AuCu_3$NRs (0.5% catalyst loading by metal atom) capped by all six different ligands and results are listed in Table 4. The initial concentration of benzonitrile was 1 mg/mL (~9.3 mM) and ultra-performance liquid chromatography (UPLC) was used to quantify the conversion by monitoring absorbance at 254 nm as listed in Tables S2 and S3. In the absence of $AuCu_3$NRs, no reaction took place at 75 °C and complete conversion from benzonitrile was observed at 95 °C after 24 h. Both of PEI600 and PEG750 capped $AuCu_3$NRs showed the highest turnover frequency and greatest conversion at either temperature among all catalysts studied. The 5000 Da PEG-capped $AuCu_3$NRs showed roughly similar, low catalytic activity, suggesting steric interference preventing access to the $AuCu_3$NR surface to catalyze the reaction. The elevated temperature provides surface lability, which reduced the graft density of the ligands. At high temperatures, the PEI10000 showed similar activity to the small ligands (i.e., PEG750 and PEI600) because the elevated temperature aided surface lability and fluidity of the ligand coating. The turnover number was found to increase by two orders of magnitude at the elevated temperature. After 24 h at 75 °C in the presence of only ligands (1 mg/mL) without $AuCu_3$NRs, no significant conversion was observed for linear polymers, while the branched ligands showed slight conversion (<5%), suggesting that the presence of the metal particles significantly enhances the rate of reaction.

In summary, we have demonstrated the effects of surface ligands on the catalytic properties of alloyed $AuCu_3$NRs. The surface anchoring group, chain length and configuration of the water-soluble, polymeric ligands were found to affect the catalytic properties of the nanoparticles. The Au-catalyzed reduction of *p*-nitrophenol was found to be detrimentally affected by thiol anchors, presumably due to the strength of the Au–thiol bond. In contrast, the Cu-catalyzed azide–alkyne cycloaddition was severely inhibited by amine functional groups because of the strong interaction between amine and Cu. Additionally, smaller ligands were found to have reduced catalytic activity relative to larger ligands owing to the decrease of graft density. From benzonitrile hydration to benzamide, elevated temperature was found to increase the mobility of ligands and result in the enhancement of catalytic activity of the ligand-capped nanocatalysts. This work reveals the potential of $AuCu_3$NRs for a variety of catalytic organic reactions, yet underscores the paramount importance of surface ligand selection in the design of nanocatalysts.

Acknowledgements

This work was funded in part by Ralph E. Powe Junior Faculty Enhancement Award, Robert C. and Sandra Connor Endowed Faculty Fellowship, and startup funds by University of Arkansas to J.C. The authors thank Prof. N. Zheng and Dr. M. Govindarajan for helpful discussions and Prof. H. Wasserman for instilling a love of science, education, and inquiry.

Supplementary data

Supplementary data associated with this article can be found, in the online version, at http://dx.doi.org/10.1016/j.tetlet.2015.03.041.

References and notes

1. Yan, N.; Xiao, C.; Kou, Y. *Coord. Chem. Rev.* **2010**, *254*, 1179–1218.
2. Polshettiwar, V.; Varma, R. S. *Green Chem.* **2010**, *12*, 743–754.
3. Wang, D.; Li, Y. *Adv. Mater.* **2011**, *23*, 1044–1060.
4. Schrinner, M.; Ballauff, M.; Talmon, Y.; Kauffmann, Y.; Thun, J.; Möller, M.; Breu, J. *Science* **2009**, *323*, 617–620.
5. Coppage, R.; Slocik, J. M.; Sethi, M.; Pacardo, D. B.; Naik, R. R.; Knecht, M. R. *Angew. Chem., Int. Ed.* **2010**, *49*, 3767–3770.
6. Biswas, M.; Dinda, E.; Rashid, M. H.; Mandal, T. K. *J. Colloid Interface Sci.* **2012**, *368*, 77–85.
7. Kameoka, S.; Tsai, A. P. *Catal. Lett.* **2008**, *121*, 337–341.
8. Chimentão, R. J.; Medina, F.; Fierro, J. L. G.; Llorca, J.; Sueiras, J. E.; Cesteros, Y.; Salagre, P. *J. Mol. Catal. A: Chem.* **2007**, *274*, 159–168.
9. Della Pina, C.; Falletta, E.; Rossi, M. *J. Catal.* **2008**, *260*, 384–386.
10. Bracey, C. L.; Ellis, P. R.; Hutchings, G. J. *Chem. Soc. Rev.* **2009**, *38*, 2231–2243.
11. Chen, S.; Jenkins, S. V.; Tao, J.; Zhu, Y.; Chen, J. *J. Phys. Chem. C* **2013**, *117*, 8924–8932.
12. Vankayala, R.; Sagadevan, A.; Vijayaraghvan, R.; Kuo, C.-L.; Hwang, K. C. *Angew. Chem., Int. Ed.* **2011**, *50*, 10640–10644.
13. Wasserman, H. H.; Ives, J. L. *Tetrahedron* **1981**, *37*, 1825–1852.
14. Wasserman, H. H.; Petersen, A. K.; Xia, M.; Wang, J. *Tetrahedron Lett.* **1999**, *40*, 7587–7589.
15. Wasserman, H. H.; McKeon, J. E.; Smith, L.; Forgione, P. *J. Am. Chem. Soc.* **1960**, *82*, 506–507.
16. Jenkins, S.; Incarvito, C. D.; Parr, J.; Wasserman, H. H. *CrystEngComm* **2009**, *11*, 242–245.
17. Yang, J.; Sargent, E.; Kelley, S.; Ying, J. Y. *Nat. Mater.* **2009**, *8*, 683–689.
18. Herves, P.; Perez-Lorenzo, M.; Liz-Marzan, L. M.; Dzubiella, J.; Lu, Y.; Ballauff, M. *Chem. Soc. Rev.* **2012**, *41*, 5577–5587.
19. Pozun, Z. D.; Rodenbusch, S. E.; Keller, E.; Tran, K.; Tang, W.; Stevenson, K. J.; Henkelman, G. *J. Phys. Chem. C* **2013**, *117*, 7598–7604.
20. Gu, S.; Wunder, S.; Lu, Y.; Ballauff, M.; Fenger, R.; Rademann, K.; Jaquet, B.; Zaccone, A. *J. Phys. Chem. C* **2014**, *118*, 18618–18625.
21. Xia, X.; Yang, M.; Zheng, Y.; Li, Q.; Chen, J.; Xia, Y. *ACS Nano* **2012**, *6*, 512–522.
22. Guisbiers, G.; Mejia-Rosales, S.; Khanal, S.; Ruiz-Zepeda, F.; Whetten, R. L.; José-Yacaman, M. *Nano Lett.* **2014**, *14*, 6718–6726.
23. Kolb, H. C.; Finn, M. G.; Sharpless, K. B. *Angew. Chem., Int. Ed.* **2001**, *40*, 2004–2021.
24. Alonso, F.; Moglie, Y.; Radivoy, G.; Yus, M. *Tetrahedron Lett.* **2009**, *50*, 2358–2362.
25. Díaz Arado, O.; Mönig, H.; Wagner, H.; Franke, J.-H.; Langewisch, G.; Held, P. A.; Studer, A.; Fuchs, H. *ACS Nano* **2013**, *7*, 8509–8515.
26. Downs, E. L.; Tyler, D. R. *Coord. Chem. Rev.* **2014**, *280*, 28–37.